Spectral Analysis of Multidimensional Stochastic Geophysical Models with an Application to Decadal ENSO Variability

RICHARD KLEEMAN

Courant Institute of Mathematical Sciences, New York, New York

(Manuscript received 6 May 2010, in final form 17 September 2010)

ABSTRACT

Simple linear models with additive stochastic forcing have been rather successful in explaining the observed spectrum of important climate variables. Motivated by this, the authors analyze the spectral character of such a general stochastic system of finite dimension. The spectral matrix is derived in the case that the spectrum is a linear combination of dynamical variables and their stochastic forcings. It is found that the most convenient basis for analysis is provided by the normal modes. In general the spectrum consists of two pieces. The first ''diagonal'' piece is a symmetric Lorentzian curve centered on the normal mode frequencies with breadth and strength determined by the normal mode dissipation. The second cross-spectrum piece derives usually from the coherency of the stochastic forcing of two different normal modes. The cross-spectrum is smaller in magnitude than the corresponding two diagonal pieces. This relative magnitude is controlled by the Wiener coherency, which is equal to the magnitude of the correlation of the stochastic forcings of different normal modes. This new analysis framework is studied in detail for the ENSO case for which a two-dimensional stochastically forced oscillator has been previously suggested as a minimal model. It is found that the observed spectrum is rather easily reproduced given appropriate dissipation. Further, it is found that the cross-spectrum results in a phase-dependent enhancement or suppression of frequencies smaller than the dominant ENSO frequency. This therefore provides a new mechanism for decadal ENSO variability. Since the cross-spectrum is phase dependent, the decadal variability generated has a distinctive spatial character. The significance of the cross-spectrum depends on the Wiener coherency, which in turn depends on the statistics of the stochastic forcing.

1. Introduction

Stochastic dynamical models are widely used in many geophysical contexts. In climate science they have been particularly influential in explaining many aspects of the low-frequency response. Perhaps the best known of such models is that of Hasselmann (1976) and Frankignoul and Hasselmann (1977), which explains the ubiquitous red spectrum of sea surface temperature (SST) using a simple linear one-dimensional Ornstein–Uhlenbeck (OU) stochastic process. The dissipation is physically related to the damping of SST by heat flux while the additive stochastic forcing originates from the influence of boundary layer turbulence on wind speed and hence heat flux. Stochastic models in the climate area have often been linear; however, important nonlinear examples also exist [e.g., ice age models (Benzi et al. 1982) or midlatitude atmospheric models (Majda et al. 2008)]. Linear models have often been multidimensional OU processes. Important examples are those explaining the spectrum of ENSO variability (e.g., Kleeman 2008b) and another that is proposed as a mechanism for midlatitude decadal variability (see Saravanan and McWilliams 1998). In both these cases one can show that the basic behavior of the stochastic model is explicable using a two-dimensional OU process (see Kleeman 2002, 2008a). Qualitatively such a system is a white noise–forced damped oscillation with the period of oscillation determined by a natural physical time scale. In the ENSO case this is simply the period of the most unstable normal mode whereas in the decadal model it is provided by the advective time scale of the midlatitude western boundary current.

Given the robust success of some of these simple stochastic models in explaining the observed spectra of climate phenomena, it would appear useful to explore the general behavior of the spectra of such systems and determine their relationship to the normal modes of the

Corresponding author address: Richard Kleeman, Courant Institute of Mathematical Sciences, 251 Mercer St., New York, NY 10012.
E-mail: kleeman@cims.nyu.edu

DOI: 10.1175/2010JAS3546.1

(unforced) linearized dynamics. This general question appears important since most dynamical systems of relevance to geophysical applications are of high dimension, and unresolved scales of motion are naturally modeled to first order by additive stochastic forcing (and additional linear damping). Of course, in certain situations the number of relevant normal modes may be small because of strong differential damping of modes.[1] On the other hand, many interesting systems have many relevant normal modes and there is no a priori reason to expect stochastic forcing to favor a very small subset of these. Naturally, for an OU process to be physically relevant one needs to assume that the linearized system is a reasonable approximation and additionally that multiplicative effects with respect to the stochastic forcing are not important to first order.

The article here is motivated by the above considerations. In section 2 we develop the general theory of the spectra of OU processes and relate it to multivariate time series analysis and classical linear resonance theory. In section 3 we give a particularly simple application that amounts to a new mechanism for the decadal variability of ENSO. Finally, section 4 contains a discussion of further potential applications as well as a summary.

2. Spectral theory of a general Ornstein–Uhlenbeck stochastic process

a. The spectrum matrix

A general multivariate Ornstein–Uhlenbeck process can be written in Langevin form as

$$\mathbf{x}_t = -\mathbf{A}\mathbf{x} + \mathbf{F}, \tag{1}$$

where the dynamics vector $\mathbf{x}$ and stochastic forcing vector $\mathbf{F}$ are of finite length n. We are assuming implicitly that $\mathbf{A}$ is constant and that the white noise forcing vector $\mathbf{F}$ has constant statistics. Note that for this system to have a statistically steady state we require that the real part of the eigenvalues of the matrix $\mathbf{A}$ are positive. Equivalently the normal modes of the associated deterministic system (i.e., the system with $\mathbf{F} = 0$) must all be damped. The spectrum matrix for the dynamical vector $\mathbf{x}$ when the system is statistically steady is well known (see Gardiner 2004, p. 111) and is given by

$$\mathbf{S}(\omega) = \frac{1}{2\pi}(\mathbf{A} + i\omega\mathbf{I})^{-1}\mathbf{R}(\mathbf{A}^* - i\omega\mathbf{I})^{-1}, \tag{2}$$

where $\mathbf{R}$ is the covariance matrix for the forcing vector $\mathbf{F}$, $\mathbf{I}$ is the identity matrix, and the star indicates an Hermitean conjugate. The significance of this matrix is that it enables us to easily calculate the usual (scalar) spectrum of any linear combination of the components of $\mathbf{x}$, namely x_j. In particular, suppose we are interested in the spectrum of the following variable:

$$y = \sum_{j=1}^{n} a_j x_j.$$

This is given by

$$S_y(\omega) = \mathbf{a}\mathbf{S}(\omega)\mathbf{a}^*.$$

It is possible to extend this spectrum matrix to include the stochastic forcing vector $\mathbf{F}$. This may be of interest when one requires the spectrum of physical variables that involve this forcing. A specific example could be tropical rainfall, where one can envisage a stochastic modeling of small-scale precipitation as a stochastic term (see, e.g., Salby and Garcia 1987) that forces dynamical variables through latent heating. The dynamical response to this causes a large-scale precipitation proportional to the low-level convergence. The total precipitation field then involves both the stochastic forcing as well as the dynamical convergence. The spectrum of total precipitation is naturally of great interest given that it is used as a central analysis tool by observationalists (see Wheeler and Kiladis 1999). Another application may be found in the stochastic modeling of the midlatitude atmosphere where the stochastic forcing is of significant interest to the dynamical analysis of the system (e.g., Newman et al. 1997). To deal with this more general situation, we introduce an extended vector of length $2n$:

$$\mathbf{z} \equiv (\mathbf{x}, \mathbf{F}).$$

The spectrum matrix of this extended random variable can then be calculated and is given by

$$\mathbf{S}(\omega) = \frac{1}{2\pi}\begin{pmatrix} \mathbf{R} & \mathbf{R}(\mathbf{A}^* - i\omega\mathbf{I})^{-1} \\ (\mathbf{A} + i\omega\mathbf{I})^{-1}\mathbf{R} & (\mathbf{A} + i\omega\mathbf{I})^{-1}\mathbf{R}(\mathbf{A}^* - i\omega\mathbf{I})^{-1} \end{pmatrix}. \tag{3}$$

Notice that the lower diagonal entry here reproduces, as expected, Eq. (2). The details of this calculation may be found in the appendix and require a rather careful and mathematically technical presentation. Also included there is a proof that this Hermitean extended spectrum matrix is nonnegative definite. This latter property ensures that all scalar spectra derived from this matrix are nonnegative.

[1] This appears to be the case for the ENSO system.

b. Normal mode and cross-spectrum analysis

Consider a basis in which $\mathbf{A}$ is diagonal (i.e., the normal mode basis).[2] Then

$$\mathbf{B} = \mathbf{G}^{-1}\mathbf{A}\mathbf{G}$$

will be diagonal and $\mathbf{G}$ will have as its columns the eigenvectors of $\mathbf{A}$. The diagonal entries of $\mathbf{B}$ are the complex eigenvalues $q_l \equiv \epsilon_l + i\eta_l$. It now follows easily that the modified Langevin equation is

$$\mathbf{y}_t = -\mathbf{B}\mathbf{y} + \mathbf{G}^{-1}\mathbf{F},$$

where $\mathbf{y} = \mathbf{G}^{-1}\mathbf{x}$. The spectrum matrix is now more easily computed since $\mathbf{B} + i\omega\mathbf{I}$ and its adjoint are diagonal. In the normal mode basis for the extended vector $\mathbf{z}$ the spectral matrix becomes

$$\mathbf{S}^N(\omega) = \frac{1}{2\pi}\begin{bmatrix} \mathbf{R}^N & \mathbf{R}^N\mathbf{D}^*\left(\dfrac{1}{q_j + i\omega}\right) \\ \mathbf{D}\left(\dfrac{1}{q_j + i\omega}\right)\mathbf{R}^N & \mathbf{D}\left(\dfrac{1}{q_j + i\omega}\right)\mathbf{R}^N\mathbf{D}^*\left(\dfrac{1}{q_j + i\omega}\right) \end{bmatrix},$$

where the stochastic forcing covariance matrix in the normal mode basis is given by

$$\mathbf{R}^N = \mathbf{G}^{-1}\mathbf{R}(\mathbf{G}^{-1})^*$$

and where the matrix $\mathbf{D}(w_l)$ is the diagonal matrix whose lth diagonal entry is w_l. Note also that when we form an inner product with $\mathbf{S}^N$ to compute the spectrum of a variable that is a linear combination of the dynamical variables and their corresponding random forcings, we do so with respect to the normal mode basis. Suppose that this linear combination is $\mathbf{u} = (\mathbf{r}, \mathbf{s})$, where the first vector is the components for the corresponding forcing while the second is the random variable components. It is easily shown (see the final proof in the appendix) that

$$\mathbf{S}_\mathbf{u} \equiv \mathbf{u}\mathbf{S}^N\mathbf{u}^* = \sum_{i,j} t_i R^N_{ij} t^*_j,$$

$$t_j \equiv r_j + \frac{s_j}{q_j + i\omega}. \tag{4}$$

It is clear that the spectrum of individual normal mode random variables is

$$S_i(\omega) = \frac{R^N_{ii}}{(\eta_i + \omega)^2 + \epsilon_i^2},$$

while that of the stochastic forcing is white, as expected. This functional form is the usual Lorentzian form seen in classical linear resonance response theory (see Landau and Lifshitz 1981, chapter 5) and indicates a spectrum peaking on the dispersion curve with a broadening due to dissipation. The peak value of this spectrum is inversely proportional to the square of the dissipation, showing the strong sensitivity of spectra of normal modes to their dissipation value. The linear combination of such random variables does not necessarily have a spectrum equal to the sum of such terms because of the cross correlation between the various normal mode forcings (i.e., a possibly nondiagonal $\mathbf{R}^N$). This results in nonzero cross-spectra between the various modes and the forcings. The cross-spectra can contribute nontrivially to the spectrum of the linear combinations. Note that in the simple (Hamiltonian) cases considered by Landau and Lifschitz cited above, such cross terms can occur between normal modes whose eigenvalues q_i are complex conjugates of each other, meaning that the spectrum is not simply the sum of two Lorentzian curves centered on $\pm\eta_i$. Indeed, if one considers the simple stochastically forced damped oscillator, the spectrum of linear combinations can range from ones in which there are peaks near $\pm\eta$ through to the case where there is a spectral peak only at $\omega = 0$, depending on which linear combination is considered and what the covariances of the stochastic forcings onto the two real components of the system are. We consider this simple case further in the next section. In the context of climate and atmospheric science, these issues have also been discussed in detail in Penland and Ghil (1993) and Penland and Matrosova (1994).

A detailed analysis of cross spectral analysis may be found in chapter 9 of Priestley (1983). The contribution to the spectra of linear combinations is actually the real

[2] For very particular choices of the matrix $\mathbf{A}$ such a diagonal basis may not exist. This occurs if two of the complex eigenvalues are exactly identical, which is of course unusual. In that case a very small perturbation may be added to $\mathbf{A}$ to ensure all eigenvalues are distinct. This enables the analysis described in this section to proceed. One can then allow this small perturbation to go to zero. More details on this method in another context can be found in Risken (1989, p. 155).

part of the complex cross-spectra. It is convenient conceptually to consider the cross-spectrum between all the normal modes and all the stochastic forcings separately. In addition, to facilitate decomposition of the desired linear combination spectrum, we multiply each normal mode and each stochastic forcing by their component in the desired combination to get

$$C_{kl}(\nu) = x_k R^N_{kl} x^*_l, \tag{5}$$

where

$$x_k = \frac{s_k}{q_k + i\omega} \quad \text{Normal Modes},$$

$$x_k = r_k \quad \text{Stochastic Forcing}.$$

Writing the cross-spectrum in polar form,

$$C_{kl}(\omega) = T_{kl}(\omega)\exp[i\theta_{kl}(\omega)],$$

we identify the usual cross-amplitude and phase spectrum (see Priestley 1983) as the real T and θ. The contribution to the desired spectrum is therefore the real part of this, namely

$$D_{kl}(\omega) = T_{kl}(\omega)\cos[\theta_{kl}(\omega)].$$

Note that it is easy to show that $\theta_{kk} = 0$ and also that this matrix is symmetric because of the Hermitean character of $\mathbf{R}^N$. The cross-amplitude spectrum can be written conveniently as

$$T_{kl} = \sqrt{C_{kk}(\omega)C_{ll}(\omega)}f_{kl}(\omega),$$

where $f_{kl}(\omega)$ is the Wiener coherence, which is the squared correlation of the random variables at frequency ω. In this particular (linear) case it is easily shown to not be frequency dependent and in fact to be the magnitude of the (complex) correlation of the normal mode stochastic forcings:

$$f_{kl} = \frac{|R^N_{kl}|}{\sqrt{R^N_{kk}R^N_{ll}}}.$$

It follows now that the desired spectrum is

$$S_{\mathbf{u}}(\omega) = \sum_{k,l}\sqrt{S_k(\omega)S_l(\omega)}f_{kl}\cos[\theta_{kl}(\omega)], \tag{6}$$

$$S_k(\omega) \equiv C_{kk}(\omega),$$

where it is clear that the S_k are simply the spectra of the projection of the linear combination onto the various normal modes and stochastic forcings. They are obviously of the form of Lorentzian functions or are constants as per the arguments above. Note that it is easy to see that the magnitude of the cross terms are always less than or equal to the sum of the corresponding diagonal S_k and S_l with equality only possible if $\cos\theta_{kl} = \pm 1$; $f_{kl} = 1$ and $S_k = S_l$. Therefore, to assess the importance of the various terms to the total spectrum it suffices to check all S_k for their contribution and then the relevant f_{kl} to check the possible importance of cross terms associated with two large diagonal contributions.

Naturally in dynamical systems where there is strong differential damping of the normal modes, which is typical in many geophysical applications, the least damped normal modes will usually strongly dominate the total spectrum because of the Lorentzian form of $S_k(\omega)$. Of course, such a conclusion depends on the stochastic forcing onto the various normal modes not varying greatly in the opposite sense (i.e., on the value of R^N_{kk} not acting in the opposite direction to ϵ_k^{-2}).

The ''diagonal'' contributors to the spectrum (6) are easily understood as being either Lorentzian functions centered on $-\eta_i$ or constants. The ''off-diagonal'' or cross-spectrum terms are a little more complex. In general it is easy to see that they may be written as

$$2\sqrt{S_kS_l}f_{kl}\cos\theta_{kl}(\omega),$$

using the Hermitean nature of the spectral matrix. It is interesting to split up the phase spectrum into pieces due to the following influences:

(i) the phase of the projection onto the normal modes (r_i or s_i) of the variable whose spectrum we seek;
(ii) a phase associated with the statistics of the stochastic forcing; and
(iii) a phase associated with the normal mode eigenvalue and the frequency.

By writing all the relevant factors in polar form, we easily obtain the following:

$$\theta_{kl}(\omega) = \theta^1_k - \theta^1_l + \theta^2_{kl} + \theta^3_k(\omega) - \theta^3_l(\omega), \tag{7}$$

where

$$\cos\theta^1_k = \frac{\text{Real}(s_k)}{|s_k|} \quad \text{or} \quad \frac{\text{Real}(r_k)}{|r_k|},$$

$$\cos\theta^2_{kl} = \frac{\text{Real}(R^N_{kl})}{|R^N_{kl}|},$$

$$\cos\theta^3_k(\omega) = \frac{\text{Real}(q_k + i\omega)}{|q_k + i\omega|} \quad \text{or} \quad 1$$

$$= \frac{\epsilon_k}{\sqrt{\epsilon_k^2 + (\eta_k + \omega)^2}} \quad \text{or} \quad 1.$$

The ''or'' cases here correspond to when one part of the cross-spectrum derives from the stochastic forcing variable rather than an OU random variable. Notice that only the third piece here can contribute to any variation of the phase spectrum with frequency. The first two pieces can be regarded as constant offsets to the phase spectrum determined by which variable one is interested in and the stochastic forcing statistics. The variation of the third piece is relatively simple in that θ_k^3 is zero when the Lorentzian peaks at $\omega = -\eta_k$ and tends to $\pi/2$ as $\omega \to \pm\infty$. Notice also that for a given frequency range, the phase spectrum tends to flatten as the dissipation increases because it tends to dominate the frequency dependence in the denominator. Finally, note that the expressions for the cosines above only determine the phase up to a sign. One needs to also check the sign of the relevant imaginary quantity to fix this [e.g., Imag(s_k) for the first case shown].

3. A simple example with application to ENSO

As was noted above, a stochastically forced damped oscillator has been proposed as an appropriate model both for ENSO and for decadal variability in the northern midlatitudes. From a mathematical viewpoint it is relatively easy to see why models such as these are potentially physically relevant. For a physical system one has a real-valued $\mathbf{A}$ in some basis and so the normal mode eigenvalues are complex conjugate pairs. If we assume that one particular normal mode has significantly less damping ϵ than other modes, then the ϵ^{-2} dependence of the normal mode spectral peak suggests that this mode will dominate the spectral response. Such a dominant complex normal mode in isolation is equivalent mathematically to a two-dimensional damped oscillator system. This situation can be argued to be applicable to the ENSO case [see Moore et al. (2003) for supporting evidence for this view]. Alternatively, the stochastic forcing may project strongly onto a particular normal mode, which becomes therefore preferentially excited. This may be the case in the North Atlantic with respect to heat flux and decadal variability (see Saravanan and McWilliams 1998). The general case for such systems has, in terms of the stochastic systems considered in the previous section, the following matrix $\mathbf{A}$:

$$\mathbf{A} = \begin{pmatrix} \epsilon & -\eta \\ \eta & \epsilon \end{pmatrix},$$

$$\epsilon = \frac{1}{\tau},$$

$$\eta = \frac{2\pi}{T},$$

where τ is the damping time of the oscillator and T is its period. The complex normal mode eigenvalues are the conjugate pair $\varepsilon \pm i\eta$. The vectors $\begin{pmatrix} 1 \\ 0 \end{pmatrix}$ and $\begin{pmatrix} 0 \\ 1 \end{pmatrix}$ represent the real orthogonal ''phases'' of the normal mode [or the two connected principal oscillation patterns (POPs); see Von Storch et al. 1988]. The covariance matrix of the stochastic forcing $\mathbf{R}$ in this basis represents the variance of the forcing onto these two phases as well as the correlation of the two forcings. It is easy to see that this correlation may be nonzero if there is large-scale coherent stochastic forcing with a pattern different to the normal mode phases. Thus, we write this matrix as

$$\mathbf{R} = c\begin{pmatrix} 1 & r\sqrt{\alpha} \\ r\sqrt{\alpha} & \alpha \end{pmatrix},$$

where r is the correlation between phase forcings, α is the (nonnegative) ratio of the variances, and c is an arbitrary positive number reflecting the overall strength of the stochastic forcing. It is trivial to calculate the change of basis matrices to the normal mode basis, and then the stochastic covariance matrix in this basis is

$$\mathbf{R}^N = \frac{c}{2}\begin{pmatrix} 1+\alpha & 1-\alpha-2ir\sqrt{\alpha} \\ 1-\alpha+2ir\sqrt{\alpha} & 1+\alpha \end{pmatrix},$$

which in turn shows that the Wiener coherence discussed in the previous section and central to the importance of the cross-spectrum between the conjugate modes is given by

$$f_{12} = \frac{\sqrt{(1-\alpha)^2 + 4r^2\alpha}}{1+\alpha}.$$

This coherence thus achieves its maximum of unity when the correlation $r = \pm 1$ or when $\alpha = 0$ and its minimum of zero when $r = 0$ and $\alpha = 1$. Thus, the cross-spectrum is strongest when the stochastic forcing projects coherently (or anticoherently) onto both phases of the normal mode or else onto one phase only and is weakest when such forcings are uncorrelated and equal in strength. A plot of the general behavior can be seen in Fig. 1.

The part of the spectrum not given by the cross-spectrum piece consists, as discussed in the previous section, of two Lorentzian components $S_{\pm}(\omega)$ of equal strength centered on $\omega = \pm\eta$ with width and strength controlled by the dissipation ϵ. Provided that ϵ is chosen appropriately, such a pattern qualitatively resembles the observed and modeled spectrum of ENSO (see Kleeman 2008b). Note that the Lorentzian curves reinforce for lower frequencies between the peaks $\pm\eta$. Of course, this does not occur to the same extent for higher frequencies leading to a ''red'' asymmetry, which is not apparent in the single Lorentzian profile.

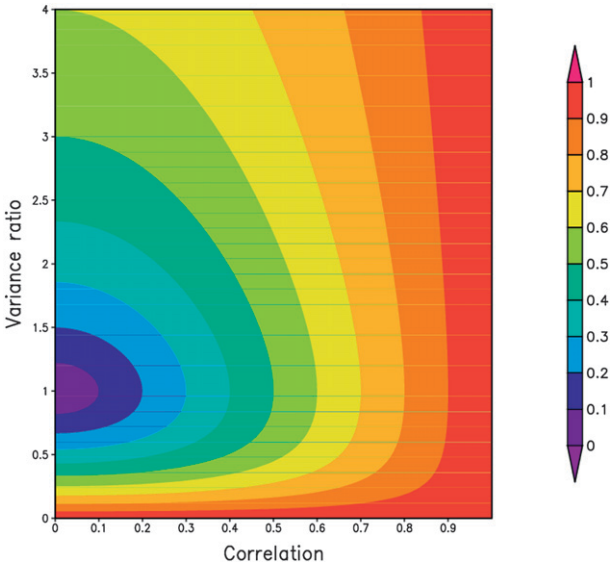

FIG. 1. The Wiener coherence for the stochastically forced damped oscillator. It is shown as a function of the correlation between the forcing onto orthogonal phases as well as the ratio of the variances of these forcings.

In addition it is interesting to calculate the cross-spectrum. The general character here depends (as discussed in the previous section) on three important (and physically independent) factors:

(i) the particular phase with respect to the normal mode for the physical variable whose spectrum we require;
(ii) the statistical character of the stochastic forcing (i.e., the variables α and r); and
(iii) the frequency dependency, which is intimately connected to the normal mode eigenvalues specifying which cross-spectrum is being considered. In the case under consideration here, of course, such eigenvalues are complex conjugates.

With respect to the first factor we require that the physical variable be written as a linear combination of the eigenvectors. A general real vector can be written uniquely as a linear combination of the normalized eigenvectors $\mathbf{v}_+$ and $\mathbf{v}_-$:

$$\begin{pmatrix} a \\ b \end{pmatrix} = \frac{a - ib}{\sqrt{2}}\mathbf{v}_+ + \frac{a + ib}{\sqrt{2}}\mathbf{v}_-,$$

$$\mathbf{v}_\pm = \frac{1}{\sqrt{2}}\begin{pmatrix} 1 \\ \pm i \end{pmatrix}.$$

Thus, in this case the projections onto the two normal modes are complex conjugates of each other and hence contribute phase angles of opposite sign; hence, by Eq. (7) the contribution to the phase spectrum is twice the phase angle with respect to the normal mode. Using the form of $\mathbf{R}^N$ derived above together with the results of the previous section, we obtain

$$C(\omega) = 2\sqrt{S_+(\omega)S_-(\omega)}f_{12} \times \cos[2\theta^1 + \theta^2 + \theta^3_+(\omega) - \theta^3_-(\omega)],$$

with

$$\cos\theta^1 = \frac{a}{\sqrt{a^2 + b^2}},$$

$$\cos\theta^2 = \frac{1 - \alpha}{\sqrt{(1 - \alpha)^2 + 4r^2\alpha}},$$

$$\cos\theta^3_+(\omega) = \frac{\epsilon}{\sqrt{\epsilon^2 + (\omega + \eta)^2}},$$

$$\cos\theta^3_-(\omega) = \frac{\epsilon}{\sqrt{\epsilon^2 + (\omega - \eta)^2}}.$$

Notice that since the normal mode phase angle is doubled (as expected), patterns of opposite sign have identical spectra and further the cross-spectrum changes sign for phases separated by $\pi/2$. Note also that the statistical properties of the forcing cause a phase shift through θ^2 similar to phase shifting with respect to the normal mode component θ^1. Their arguably more important effect is through alteration of the Wiener coherence f_{12}, which controls the relative magnitude of the cross-spectrum to the diagonal Lorentzian spectra. To simplify further discussion we nondimensionalize the time scale by $T/2\pi$, meaning that η is set to unity. After discarding the common factor of $(1 + \alpha)(a^2 + b^2)$ between diagonal and cross-spectral components, we obtain the functional forms

$$C'(\omega) = \frac{2f_{12}\cos[\theta^3(\omega) - \gamma]}{\sqrt{[\epsilon^2 + (\omega - 1)^2][\epsilon^2 + (\omega + 1)^2]}},$$

$$\theta^3(\omega) = \theta^3_+(\omega) - \theta^3_-(\omega),$$

$$S_\pm(\omega) = \frac{1}{\epsilon^2 + (\omega \pm 1)^2},$$

$$S(\omega) = S_+(\omega) + C'(\omega) + S_-(\omega),$$

where the angle γ is adjustable according to which variable one wishes to analyze spectrally. It is clear that the phase spectrum is simply $\theta^3(\omega)$ with an arbitrary offset

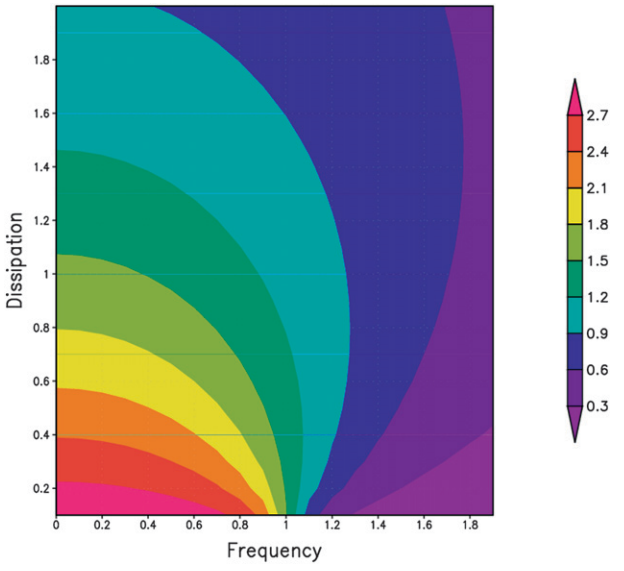

FIG. 2. The phase spectrum as a function of frequency and dissipation (nondimensionalized by $2\pi/T$, where T is the normal mode period).

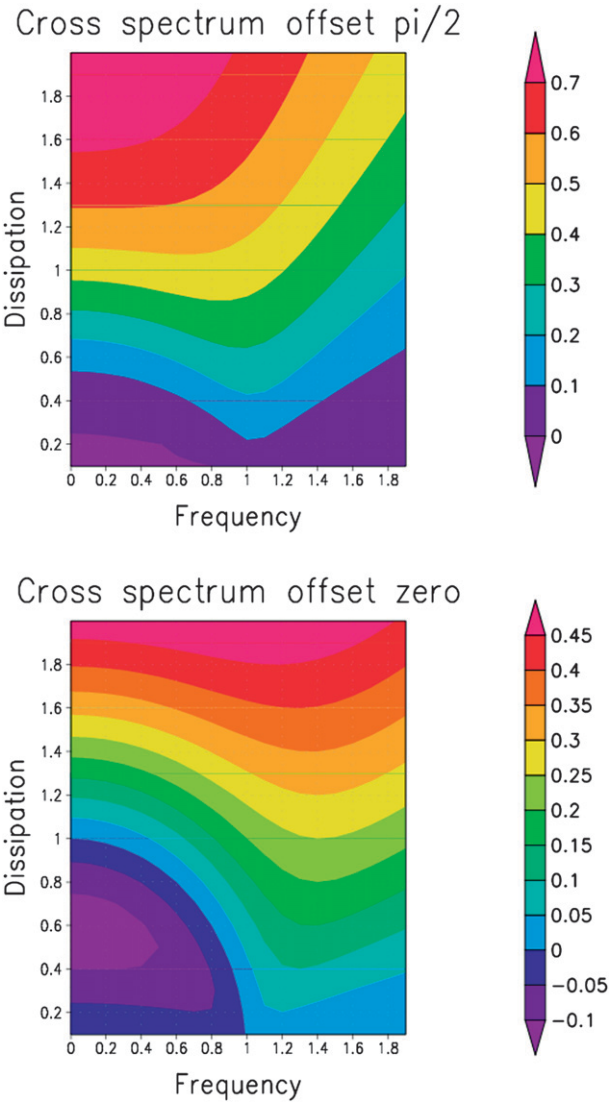

FIG. 3. The cross-spectrum as a function of the variables in Fig. 2. Note that it has been multiplied by a factor of ϵ^2 in order to see the relative strength compared with the diagonal Lorentzian spectrum, which has a peak value of ϵ^{-2}.

angle that depends only on the forcing statistics and the particular normal mode phase under consideration. This is shown as a function of frequency and dissipation in Fig. 2. It is clear that the degree of variation with frequency drops significantly as the dissipation increases, as was noted analytically in the previous section. The cross-spectrum is shown as a function of the same variables in Fig. 3 for various offset angles that correspond to a variety of phases of the normal mode. The cross-spectrum has been multiplied by the Lorentzian peak value of ϵ^{-2} in order to show the relative weight. For values of the dissipation around unity (which gives a reasonable fit to observations by the diagonal spectrum), it is clear that for certain offset phases there is a differential strengthening of the low-frequency spectrum relative to the high-frequency piece. This implies that if the Wiener coherence is significantly nonzero, then certain phases of the normal mode may have enhanced low-frequency power compared with others. Indeed, it is easy to see that contributions of this type of opposite sign are separated by a normal mode phase angle of $\pi/2$.

If we take this very simple model seriously, in the ENSO context this implies that the various phases of ENSO may have differing spectral characters in the low-frequency range, with the biggest difference occurring with a time separation of a little less than a year because that corresponds with a phase change of $\pi/2$. Additionally, since the various ENSO phases have very distinctive spatial characters, one would expect this cross-spectral effect to result in a distinct spatial structure for decadal variations, as indeed is observed (e.g., Latif et al. 1997; Zhang et al. 1997). The potential difference in the total spectrum is shown in Fig. 4a, which is the total spectrum at phase differences of $\pi/2$ with respect to the ENSO cycle. Values of $\epsilon = 0.8$ and a Wiener coherence of 0.1 were selected. Notice how the low-frequency enhancement is reasonably uniform for frequencies extending from the peak to zero. Also shown in Fig. 5 for reference is the dependency of the spectrum on dissipation (the lower curve phase lag of Fig. 5 was chosen). This sensitivity is quite strong, suggesting that realistic values of the dissipation lie in the range of 0.7–1.0, which implies a damping time scale of around 8–11 months. Such a result has been

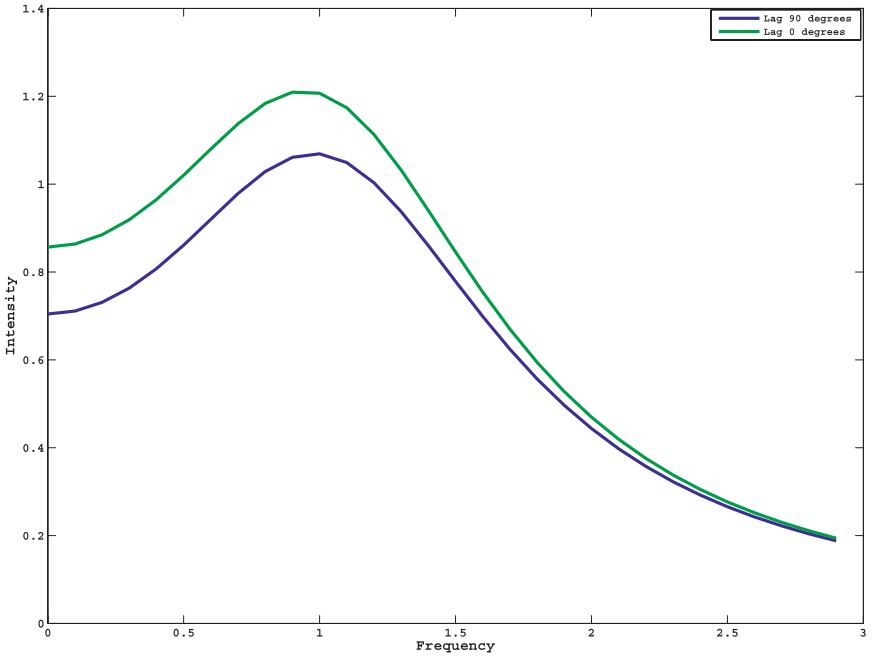

FIG. 4. The variation in the total spectrum with respect to normal mode phase. The two curves are separated by a phase of $\pi/2$ and have dissipation of 0.8.

deduced previously using Markov modeling of SST by Penland and Matrosova (1994) and has important consequences for ENSO predictability limits (e.g., Thompson and Battisti 2001).

Extension to nonnormal models

It has been argued on the basis of statistical modeling of observations (e.g., Penland and Sardeshmukh 1995; Penland and Matrosova 2006) and from skillful ENSO coupled dynamical models (e.g., Moore and Kleeman 1999; Moore et al. 2003) that nonnormal effects are important to ENSO, particularly on time scales of several months where growing singular vectors may be important. Since the very simple model above is normal, it is interesting to examine the consequences of nonnormality to the steady-state spectrum. The most straightforward way to deal with this, within the normal mode formalism presented here, is to add further complex normal modes with increasing damping rates. In addition, one could incorporate nonorthogonality of such modes (and the original primary mode). Both of these effects lead to nonnormality and have been noted in the studies mentioned above. An examination of the observed ENSO spectrum (see Kleeman 2008b) reveals that it is rather easy to get a reasonable fit using the previous model since there is a dominant peak with an approximately Lorentzian decay about this. The additional normal modes seen in the previous studies above tend to often have rather different frequencies to the dominant mode, which would suggest that their (steady state) spectral contribution may not be large. There may be two different reasons for this. First, the additional modes are likely more highly damped and the spectral peak strength varies strongly as the square of decay time. Second, spectral strength also depends on the diagonal values R_{ii}^N and these values are influenced by the projection character of the stochastic forcing onto the modes as well as by their orthogonality properties. It may be that this diagonal value is not large for reasons of both the statistics of the stochastic forcing and the dynamics that control the nonorthogonality. These issues deserve a further detailed study using the formalism described above. This is currently in progress.

4. Summary and discussion

Simple linear systems with additive stochastic forcing have proven to be useful models for the ubiquity of low-frequency climate variability (Hasselmann 1976; Kleeman 2002; Saravanan and McWilliams 1998). In particular, they explain rather well the spectral character of many SST time series. This motivates the analysis of the spectrum of a general such process, which is referred to in the mathematics literature as a multivariate Ornstein–Uhlenbeck (OU) process. In this contribution we have derived a framework for analyzing the spectrum of a general such process of finite dimension. It is found that a normal mode basis is most convenient for the analysis

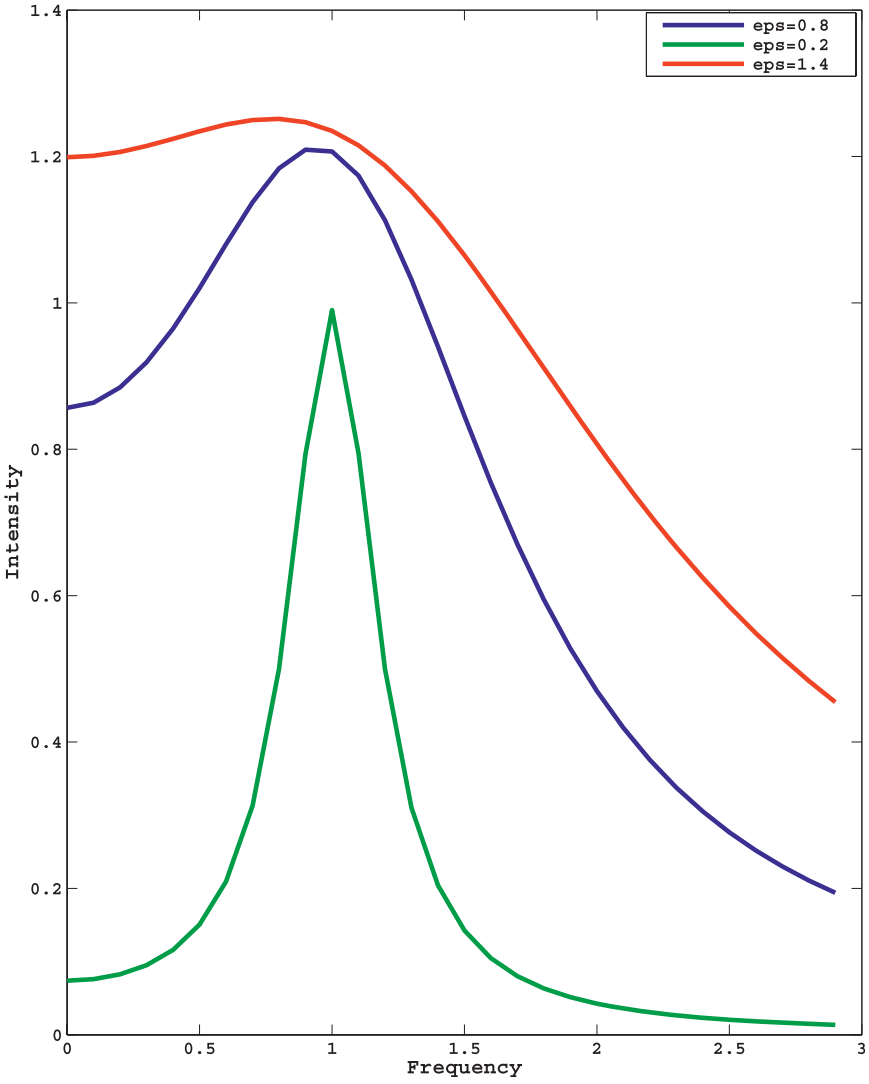

FIG. 5. The dependency of the total spectrum on dissipation. Shown (in order of strength after multiplication by ϵ^2) are $\epsilon = 0.2$, $\epsilon = 0.8$, and $\epsilon = 1.4$.

since this allows for an explicit evaluation of the spectral matrix in terms of the dynamically significant normal mode eigenvalues.

We considered the spectra of a general linear combination of OU random variables and the OU stochastic forcings. The spectrum of such linear combinations consists of two broad pieces:

(i) ''Diagonal'' terms, which take the form either of Lorentzian functions (see Landau and Lifshitz 1981) centered on normal mode frequencies (with breadth and intensity controlled by the normal mode dissipation) or else constant terms. Which of these is important is determined by the particular linear combination being considered. The Lorentzian functions are important when there is significant projection of the linear combination of OU random variables onto a particular normal mode; the constant terms are important if there is projection from the linear combination onto a particular (normal mode) stochastic forcing.

(ii) ''Off-diagonal'' terms, which are the cross-spectra of the various normal modes and normal mode forcings. These cross-spectra always contribute at an amplitude less than the sum of the two diagonal spectra since they can be written in the form

$$C(\omega) = 2\sqrt{S_1 S_2} f_{12} \cos\theta(\omega),$$

where the diagonal spectra are S_1 and S_2. The nonnegative Wiener coherence f_{12} is simply the magnitude

of the correlation of the stochastic forcings of each normal mode and so never exceeds unity and only depends on the stochastic forcing statistics. Finally, the phase spectrum $\theta(\omega)$ in general depends in a nontrivial way on the (complex) normal mode eigenvalues.

It is hoped that this general framework will prove useful in analyzing situations where linearization is a good approximation and many normal modes are important in explaining the underlying dynamics. Potential examples include the midlatitude atmosphere (e.g., DelSole and Farrell 1995; Zhang and Held 1999) or tropical convection (e.g., Wheeler and Kiladis 1999).

It should also serve to generalize existing simple stochastic climate models to more complicated situations. As a first step in this direction, the two-dimensional ENSO case was analyzed in considerable detail. The dynamics here are of a decaying oscillation intended to represent the dominant (least dissipated) normal mode of the Pacific coupled atmosphere–ocean system. The two real components of this system correspond with the independent phases of the ENSO and correspond with the first two EOFs of ocean heat content (and their associated patterns in other physical variables). The diagonal spectrum for this particular case agrees qualitatively with the observed ENSO spectrum (see Kleeman 2008b), provided that the dissipation is chosen to have a time scale somewhat less than a year. The cross-spectrum acts primarily to enhance or suppress the total spectrum with periods greater than that of the normal mode oscillation (i.e., around four years). This enhancement or suppression depends on the phase of ENSO chosen to spectrally analyze with maximal enhancement occurring one-quarter of a cycle before maximum suppression. Thus, if the cross-spectrum is important, then one would expect to see a spatial dependency on the low-frequency range of ENSO, as indeed is observed. The reason for the appearance of this low-frequency effect lies in the fact that this two-dimensional model has two natural time scales originating from the real and imaginary part of the normal mode eigenvalue and corresponding with the oscillation period and its damping time.

Whether the cross-spectrum is significant or not depends crucially on the Wiener coherence f_{12}, and this in turn depends on the statistics of the stochastic forcing. In particular, coherence between the forcing of the various phases enhances f_{12} as does unequal variances for these different phases. It is believed (see Kleeman 2008b) that a significant part of the stochastic forcing is provided by atmospheric convective transients and it is well known that these have most power at low wavenumbers (see Wheeler and Kiladis 1999). This is consistent with at least a small amount of phase coherency for the stochastic forcing. It is important to study this issue further within the context of a quite careful statistical analysis of estimates of the ENSO stochastic forcing [e.g., the dataset of Zavala-Garay et al. (2003)]. This is beyond the scope of the present work, which is theoretical in emphasis.

Finally, it is useful to place the current mechanism within the context of other proposed mechanisms of ENSO decadal variability. There have been a number of studies that have, like the present work, discussed decadal variability in a stochastically forced multivariate linear damped dynamical system (e.g., Penland and Matrosova 1994; Kleeman and Moore 1999; Flügel et al. 2004). The first discusses the general spectral properties of ENSO flowing from an observation-based normal mode decomposition of tropical Pacific SST. The second concentrates primarily on the decadal variation of predictability and argues that the amplitude of the dominant normal mode controls predictability and that this amplitude has strong decadal power. Finally, the third reference argues that decadal variations in the (sample) statistics of the stochastic forcing can cause decadal variability. The emphasis there was, as in the second reference, primarily but not exclusively on variations in predictability. The general framework for decomposing the complete spectrum matrix for a general OU process introduced in section 2 allows us to discuss possible connections with the present mechanism. Clearly decadal power can arise in many different ways. Most simply it is just the low-frequency end of the spectrum of the dominant normal mode, which resembles the ENSO cycle. It may also arise from significant projection onto normal modes with low/decadal frequency. It can arise through the (differential) diagonal spectral contributions of modes with different frequencies since these are associated with different spatial patterns. It could arise, as discussed here, from the internal cross-spectrum of the dominant (least damped) normal mode or from the cross-spectrum between the dominant mode and other more damped modes. Finally, if one is interested in certain quadratic quantities, such as the dominant normal mode (squared) amplitude, then decadal variability may arise through nonlinear modifications of the effects discussed here. Recall that we are only focusing here on the spectra of linear combinations of the dynamical variables. Clearly there are many possibilities and the general framework outlined here offers a way to discriminate between the many possible effects. It would be very interesting to study the dynamical and statistical models used in the above references in this way in order to discriminate between the possibilities outlined above.

Acknowledgments. The author gratefully acknowledges the generous long-term support of the National Science

Foundation and most particularly the financial support of Grant ATM-2574200. The detailed comments of three referees are also appreciated as they resulted in a significantly improved manuscript.

APPENDIX

The Extended Spectrum Matrix

The Ornstein–Uhlenbeck (OU) stochastic process considered in Eq. (1) can be written in standard rigorous Ito form (see Gardiner 2004, chapter 4) as

$$d\mathbf{x} = -\mathbf{A}\mathbf{x}\,dt + \mathbf{B}\,d\mathbf{W}, \tag{A1}$$

where the matrices $\mathbf{A}$ and $\mathbf{B}$ are constant and $\mathbf{W}$ is a standard vector Wiener process. Because $\mathbf{B}$ is a constant, the Stratonovich process

$$d\mathbf{x} = -\mathbf{A}\mathbf{x}\,dt + \mathbf{B} \circ d\mathbf{W}$$

is an identical stochastic process (see Gardiner 2004, section 4.3.6). Associated with this continuous process is a discrete process:

$$\mathbf{x}_{m+1} - \mathbf{x}_m = -\mathbf{A}\mathbf{x}_m \Delta t + \mathbf{B}\Delta\mathbf{W}_m, \tag{A2}$$

where the integer time index is specified by m and Δt represents the unit time interval. Note that the Wiener increments $\Delta\mathbf{W}_m$ here are independent random variables for different time indices m.

The discrete associated process (A2) is referred to sometimes in the introduction of the Ito calculus as the Cauchy–Euler construction (Gardiner 2004, section 4.3.1) or, in contexts where it is used as a numerical approximation to the continuous process, as the Euler–Murayama approximation (Kloeden and Platen 1992). The second reference proves that as the time grid spacing Δt is reduced to zero the discrete process converges to the associated Ito continuous process (A1). It is also worth reiterating the well-known fact (e.g., Kloeden and Platen 1992, chapter 6) that the continuous stochastic process represents a mathematical idealization since in realistic physical applications the stochastic forcing has a nonzero but ''very small'' temporal decorrelation time. Thus, on time scales shorter than this decorrelation time the continuous process is questionable physically and likely no ''better'' than an interpolated discrete process with Δt chosen appropriately. Naturally such scales are usually of little interest in stochastic modeling and the mathematical convenience of the idealized limit is strong. The reason for considering the discrete process here is that it allows us to introduce the concept of stochastic forcing in a manner that is, in our view, both precise and intuitive. With this definition we are then able to deduce associated continuous spectral properties via the time grid limiting procedure mentioned above.

In particular, we define the stochastic forcing $\mathbf{f}_m$ for the discrete system by the identification

$$\Delta t\mathbf{f}_m \equiv \mathbf{B}\Delta\mathbf{W}_m.$$

By the usual Wiener increment properties this random variable has zero mean and the following covariance:

$$\langle \mathbf{f}_k, \mathbf{f}_l^* \rangle = \frac{\delta_{kl}}{\Delta t}\mathbf{R},$$

$$\mathbf{R} \equiv \mathbf{B}\mathbf{B}^*,$$

where $\mathbf{R}$ is real and symmetric and we refer to it in the text above as the continuous stochastic forcing covariance matrix. Equation (A2) can be easily solved exactly from a specified deterministic initial condition. Since we are interested in the statistically steady case, we initialize at zero at time $-\infty$, in which case the solution becomes

$$\mathbf{x}_j = \sum_{k=0}^{\infty} \mathbf{P}^k \mathbf{f}_{j-k-1}, \tag{A3}$$

where the matrix $\mathbf{P}$ is easily seen to be given by

$$\mathbf{P} = \mathbf{I} - \Delta t\mathbf{A}.$$

Suppose we consider a fixed time interval $\tau = n\Delta t$ and consider the continuum limit $\Delta t \to 0$ and hence $n \to \infty$. It is easily derived then from standard exponential limits that

$$\lim_{\Delta t \to \infty} \mathbf{P}^n = \exp(-\mathbf{A}t). \tag{A4}$$

Note also that the matrix $\mathbf{P}^n$ here is the discrete time propagator of the system over a time interval of $\tau = n\Delta t$. In the continuum limit this becomes the usual continuous propagator seen on the right-hand side of (A4). In taking this limit we are making the implicit time identification:

$$\mathbf{x}_n \leftrightarrow \mathbf{x}(n\Delta t) = \mathbf{x}(\tau).$$

Consider now the following extended random vector:

$$\mathbf{z}_k \equiv (\mathbf{f}_k, \mathbf{x}_k),$$

which consists of both the stochastic forcing and dynamical variable of the discrete stochastic process.

Using the solution (A3) we can easily calculate the discrete time lagged covariance matrix of this augmented vector:

$$\mathbf{H}(k-l) \equiv \langle \mathbf{z}_k, \mathbf{z}_l^* \rangle = \begin{pmatrix} 0 & 0 \\ \mathbf{P}^{k-l-1}\mathbf{R} & \mathbf{P}^{k-l}\boldsymbol{\sigma} \end{pmatrix} \quad k > l$$

$$= \begin{pmatrix} \frac{1}{\Delta t}\mathbf{R} & 0 \\ 0 & \boldsymbol{\sigma} \end{pmatrix} \quad k = l \quad \text{(A5)}$$

$$= \begin{bmatrix} 0 & \mathbf{R}(\mathbf{P}^*)^{l-k-1} \\ 0 & \boldsymbol{\sigma}(\mathbf{P}^*)^{l-k} \end{bmatrix} \quad k < l, \quad \text{(A6)}$$

where $\boldsymbol{\sigma} \equiv \langle \mathbf{x}_m, \mathbf{x}_m^* \rangle$ is the steady nonlagged covariance matrix of the discrete process. As is well known, the Wiener–Khintchine theorem (see Risken 1989, p. 29; Priestley 1983, p. 225) asserts that the Fourier transform of the time-lagged covariance matrix is the corresponding spectral matrix of the random variable vector. This holds for both the discrete case and the continuous case provided that the appropriate Fourier transform is used. Taking the discrete Fourier transform of $\mathbf{H}$, we obtain the spectrum matrix for the discrete process:

$$\mathbf{s}(\omega) = \frac{1}{2\pi} \sum_{m=-\infty}^{m=\infty} \exp(-i\omega m \Delta t)\mathbf{H}(m).$$

While this is the exact spectrum matrix for the discrete process, the complicated form of (A6) makes its evaluation as a closed form expression difficult except in special cases. On the other hand, if we multiply this spectrum by Δt and take the continuum limit discussed in connection with Eq. (A4) above, then we obtain the continuous Fourier transform of the continuous time-lagged covariance matrix, which is the desired continuous spectrum matrix $\mathbf{S}(\omega)$ for the OU process. Using (A6) and taking this limit we obtain, using (A4), that this matrix is explicitly

$$\mathbf{S}(\omega) = \frac{1}{2\pi}\begin{bmatrix} \mathbf{R} & \mathbf{C}_-(\omega) \\ \mathbf{C}_+(\omega) & \mathbf{F}_-(\omega) + \mathbf{F}_+(\omega) \end{bmatrix},$$

with

$$\mathbf{C}_-(\omega) \equiv \int_{-\infty}^{0} \mathbf{R} \exp[-(i\omega + \mathbf{A}^*)\tau]\, d\tau,$$

$$\mathbf{C}_+(\omega) \equiv \int_{0}^{\infty} \exp[-(i\omega + \mathbf{A})\tau]\mathbf{R}\, d\tau,$$

$$\mathbf{F}_-(\omega) \equiv \int_{-\infty}^{0} \boldsymbol{\sigma} \exp[-(i\omega + \mathbf{A}^*)\tau]\, d\tau,$$

$$\mathbf{F}_+(\omega) \equiv \int_{0}^{\infty} \exp[-(i\omega + \mathbf{A})\tau]\boldsymbol{\sigma}\, d\tau.$$

After performing the appropriate Fourier transforms and some algebraic manipulation detailed in Gardiner (2004, p. 111), we obtain the matrix specified in Eq. (3). It should be emphasized that the continuous limit for this matrix derived here is only approximately proportional to the discrete version and for Δt sufficiently large there may be relevant differences. These might be of interest for certain discrete stochastic applications (see Kloeden and Platen 1992, chapters 6 and 7).

We now demonstrate that the matrix $\mathbf{S}(\omega)$ defined by Eq. (3) is nonnegative definite. We prove that its transpose has this property, so therefore it does also (see Horn and Johnson 1990, p. 397). Consider a general complex vector $\mathbf{x}$; we need to show that

$$\mathbf{x}^*\mathbf{S}^t\mathbf{x} \geq 0.$$

The left-hand side is easily shown to be equal to the complex inner product

$$I = (\mathbf{S}\mathbf{y}, \mathbf{y}),$$

where $\mathbf{y}$ is just the complex conjugate of $\mathbf{x}$. Splitting the extended $\mathbf{y}$ into its two pieces $\mathbf{r}$ and $\mathbf{s}$, the above inner product becomes the following sum of four inner products over a space of one-half the dimension:

$$2\pi I = (\mathbf{R}\mathbf{r}, \mathbf{r}) + (\mathbf{Q}^*\mathbf{R}\mathbf{Q}\mathbf{s}, \mathbf{s}) + (\mathbf{Q}^*\mathbf{R}\mathbf{r}, \mathbf{s}) + (\mathbf{R}\mathbf{Q}\mathbf{s}, \mathbf{r}),$$

where $\mathbf{Q} \equiv (\mathbf{A}^* - i\omega\mathbf{I})^{-1}$. Since $\mathbf{R}$ is the covariance matrix for the stochastic forcing, it is nonnegative definite and can thus be written as the product $\mathbf{P}^*\mathbf{P}$. Shuffling operators, $2\pi I$ becomes

$$2\pi I = (\mathbf{P}\mathbf{r}, \mathbf{P}\mathbf{r}) + (\mathbf{P}\mathbf{Q}\mathbf{s}, \mathbf{P}\mathbf{Q}\mathbf{s}) + (\mathbf{P}\mathbf{r}, \mathbf{P}\mathbf{Q}\mathbf{s}) + (\mathbf{P}\mathbf{Q}\mathbf{s}, \mathbf{P}\mathbf{r})$$
$$= \|\mathbf{P}\mathbf{r} + \mathbf{P}\mathbf{Q}\mathbf{s}\|^2 \geq 0.$$

REFERENCES

Benzi, R., G. Parisi, A. Sutera, and A. Vulpiani, 1982: Stochastic resonance in climatic change. *Tellus,* **34,** 10–16.

DelSole, T., and B. F. Farrell, 1995: A stochastically excited linear system as a model for quasigeostrophic turbulence: Analytic results for one- and two-layer fluids. *J. Atmos. Sci.,* **52,** 2531–2547.

Flügel, M., P. Chang, and C. Penland, 2004: The role of stochastic forcing in modulating ENSO predictability. *J. Climate,* **17,** 3125–3140.

Frankignoul, C., and K. Hasselmann, 1977: Stochastic climate models. Part II. Application to sea-surface temperature anomalies and thermocline variability. *Tellus,* **29,** 289–305.

Gardiner, C. W., 2004: *Handbook of Stochastic Methods for Physics, Chemistry, and the Natural Sciences*. Springer Series in Synergetics, Vol. 13, Springer, 415 pp.

Hasselmann, K., 1976: Stochastic climate models. Part I. Theory. *Tellus,* **28,** 473–485.

Horn, R., and C. Johnson, 1990: *Matrix Analysis*. Cambridge University Press, 575 pp.

Kleeman, R., 2002: Measuring dynamical prediction utility using relative entropy. *J. Atmos. Sci.,* **59,** 2057–2072.

——, cited 2008a: Stochastic climate models. [Available online at http://www.math.nyu.edu/faculty/kleeman/stochastic.ppt.]

——, 2008b: Stochastic theories for the irregularity of ENSO. *Philos. Trans. Roy. Soc.,* **366A,** 2509–2524.

——, and A. M. Moore, 1999: A new method for determining the reliability of dynamical ENSO predictions. *Mon. Wea. Rev.,* **127,** 694–705.

Kloeden, P. E., and E. Platen, 1992: *Numerical Solution of Stochastic Differential Equations*. Applications of Mathematics Series, Vol. 23, Springer, 636 pp.

Landau, L., and E. Lifshitz, 1981: *Mechanics*. Vol. 1, 3rd ed. *Course of Theoretical Physics,* Reed Educational, 173 pp.

Latif, M., R. Kleeman, and C. Eckert, 1997: Greenhouse warming, decadal variability, or El Niño? An attempt to understand the anomalous 1990s. *J. Climate,* **10,** 2221–2239.

Majda, A. J., C. Franzke, and B. Khouider, 2008: An applied mathematics perspective on stochastic modelling for climate. *Philos. Trans. Roy. Soc. London,* **366A,** 2427–2453.

Moore, A. M., and R. Kleeman, 1999: The nonnormal nature of El Niño and intraseasonal variability. *J. Climate,* **12,** 2965–2982.

——, J. Vialard, A. Weaver, D. L. T. Anderson, R. Kleeman, and J. R. Johnson, 2003: The role of air–sea interaction in controlling the optimal perturbations of low-frequency tropical coupled ocean–atmosphere modes. *J. Climate,* **16,** 951–968.

Newman, M., P. D. Sardeshmukh, and C. Penland, 1997: Stochastic forcing of the wintertime extratropical flow. *J. Atmos. Sci.,* **54,** 435–455.

Penland, C., and M. Ghil, 1993: Forecasting Northern Hemisphere 700-mb geopotential height anomalies using empirical normal modes. *Mon. Wea. Rev.,* **121,** 2355–2372.

——, and L. Matrosova, 1994: A balance condition for stochastic numerical models with applications to the El Niño–Southern Oscillation. *J. Climate,* **7,** 1352–1372.

——, and P. Sardeshmukh, 1995: The optimal growth of tropical sea surface temperature anomalies. *J. Climate,* **8,** 1999–2024.

——, and L. Matrosova, 2006: Studies of El Niño and interdecadal variability in tropical sea surface temperatures using a nonnormal filter. *J. Climate,* **19,** 5796–5815.

Priestley, M., 1983: *Spectral Analysis and Time Series*. Vols. 1 and 2, Academic Press, 890 pp.

Risken, H., 1989: *The Fokker–Plank Equation*. 2nd ed. Springer-Verlag, 474 pp.

Salby, M., and R. Garcia, 1987: Transient response to localized episodic heating in the tropics. Part I: Excitation and short-time near-field behavior. *J. Atmos. Sci.,* **44,** 458–498.

Saravanan, R., and J. McWilliams, 1998: Advective ocean–atmosphere interaction: An analytical stochastic model with implications for decadal variability. *J. Climate,* **11,** 165–188.

Thompson, C. J., and D. S. Battisti, 2001: A linear stochastic dynamical model of ENSO. Part II: Analysis. *J. Climate,* **14,** 445–466.

Von Storch, H., T. Bruns, I. Fischer-Bruns, and K. Hasselmann, 1988: Principal oscillation pattern analysis of the 30- to 60-day oscillation in general circulation model equatorial troposphere. *J. Geophys. Res.,* **93** (D9), 11 022–11 036.

Wheeler, M., and G. Kiladis, 1999: Convectively coupled equatorial waves: Analysis of clouds and temperature in the wavenumber–frequency domain. *J. Atmos. Sci.,* **56,** 374–399.

Zavala-Garay, J., A. Moore, C. L. Perez, and R. Kleeman, 2003: The response of a coupled model of ENSO to observed estimates of stochastic forcing. *J. Climate,* **16,** 2827–2842.

Zhang, Yuan, J. Wallace, and D. Battisti, 1997: ENSO-like interdecadal variability: 1900–93. *J. Climate,* **10,** 1004–1020.

Zhang, Yunqing, and I. Held, 1999: A linear stochastic model of a GCM's midlatitude storm tracks. *J. Atmos. Sci.,* **56,** 3416–3435.